ACS APPLIED MATERIALS & INTERFACES

Forum Article

www.acsami.org

# Polydopamine-Based 3D Colloidal Photonic Materials: Structural Color Balls and Fibers from Melanin-Like Particles with Polydopamine Shell Layers

Michinari Kohri,*[,†] Kenshi Yanagimoto,[†] Ayaka Kawamura,[†] Kosuke Hamada,[†] Yoshihiko Imai,[‡] Takaichi Watanabe,[‡] Tsutomu Ono,[‡] Tatsuo Taniguchi,[†] and Keiki Kishikawa[†]

[†]Division of Applied Chemistry and Biotechnology, Graduate School of Engineering, Chiba University, 1-33 Yayoi-cho, Inage-ku, Chiba 263-8522, Japan

[‡]Department of Applied Chemistry and Biotechnology, Graduate School of Natural Science and Technology, Okayama University, 3-1-1 Tsushima-naka, Kita-ku, Okayama 700-8530, Japan

Supporting Information

**ABSTRACT:** Nature creates beautiful structural colors, and some of these colors are produced by nanostructural arrays of melanin. Polydopamine (PDA), an artificial black polymer produced by self-oxidative polymerization of dopamine, has attracted extensive attention because of its unique properties. PDA is a melanin-like material, and recent studies have reported that photonic materials based on PDA particles showed structural colors by enhancing color saturation through the absorption of scattered light. Herein, we describe the preparation of three-dimensional (3D) colloidal photonic materials, such as structural color balls and fibers, from biomimetic core−shell particles with melanin-like PDA shell layers. Structural color balls were prepared through the combined use of membrane emulsion and heating. We also demonstrated the use of microfluidic emulsification and solvent diffusion for the fabrication of structural color fibers. The obtained 3D colloidal materials, i.e., balls and fibers, exhibited angle-independent structural colors due to the amorphous assembly of PDA-containing particles. These findings provide new insight for the development of dye-free technology for the coloration of various 3D colloidal architectures.

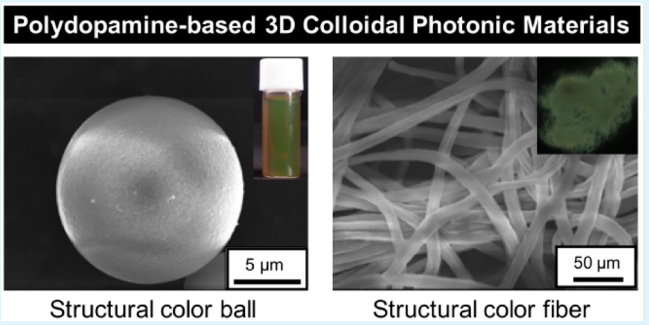


**KEYWORDS:** *polydopamine, structural color, photonic materials, membrane emulsification, microfluidics*

## INTRODUCTION

The functionalization of material surfaces is an attractive topic in material science due to its scientific significance and numerous potential applications. A simple and universal modification technique is required for the development of functional materials. In 2007, Lee and Messersmith et al. reported a creative surface modification technique using polydopamine (PDA), which was inspired by Mussel adhesive proteins.[1] A PDA layer is easily prepared by oxidative self-polymerization of dopamine hydrochloride (2-(3,4-dihydroxyphenyl)ethylamine hydrochloride) under basic conditions on a variety of materials, such as polymer materials, inorganic materials, and metals.[1] Extensive studies have been conducted to create PDA-coated materials, driven by its simple and universal deposition route, for multifunctional coatings.[2−23] We have reported the preparation of colorless PDA layers containing functional groups, i.e., atom transfer radical polymerization initiating groups,[24,25] polyethylene glycol moieties,[26] dyes,[27] carboxylic acid-bearing compounds,[28] and silane coupling reagents,[29] to produce functional polymeric materials.[30]

While most studies in which a PDA layer is used have involved modification of the material's surface, there are a limited number of reports on the use of PDA as a photonic material. In 2015, we reported for the first time the structural colors from the assembly of relatively monodisperse PDA particles.[31] Wu et al. reported the preparation of structural color materials by constructing hierarchically structured materials composed of PDA thin film and amorphous PDA particles.[32] Xiao et al. reported structurally colored films from PDA particle assemblies, and the colors were controlled by the thickness of the assembled PDA particles.[33,34] Cho et al. demonstrated the usability of PDA particle assemblies for an anticounterfeiting application.[35] Recently, we have also designed and synthesized core−shell type particles composed

**Special Issue:** 10 Years of Polydopamine: Current Status and Future Directions

**Received:** March 9, 2017
**Accepted:** June 20, 2017


© XXXX American Chemical Society

DOI: 10.1021/acsami.7b03453
*ACS Appl. Mater. Interfaces* XXXX, XXX, XXX−XXX

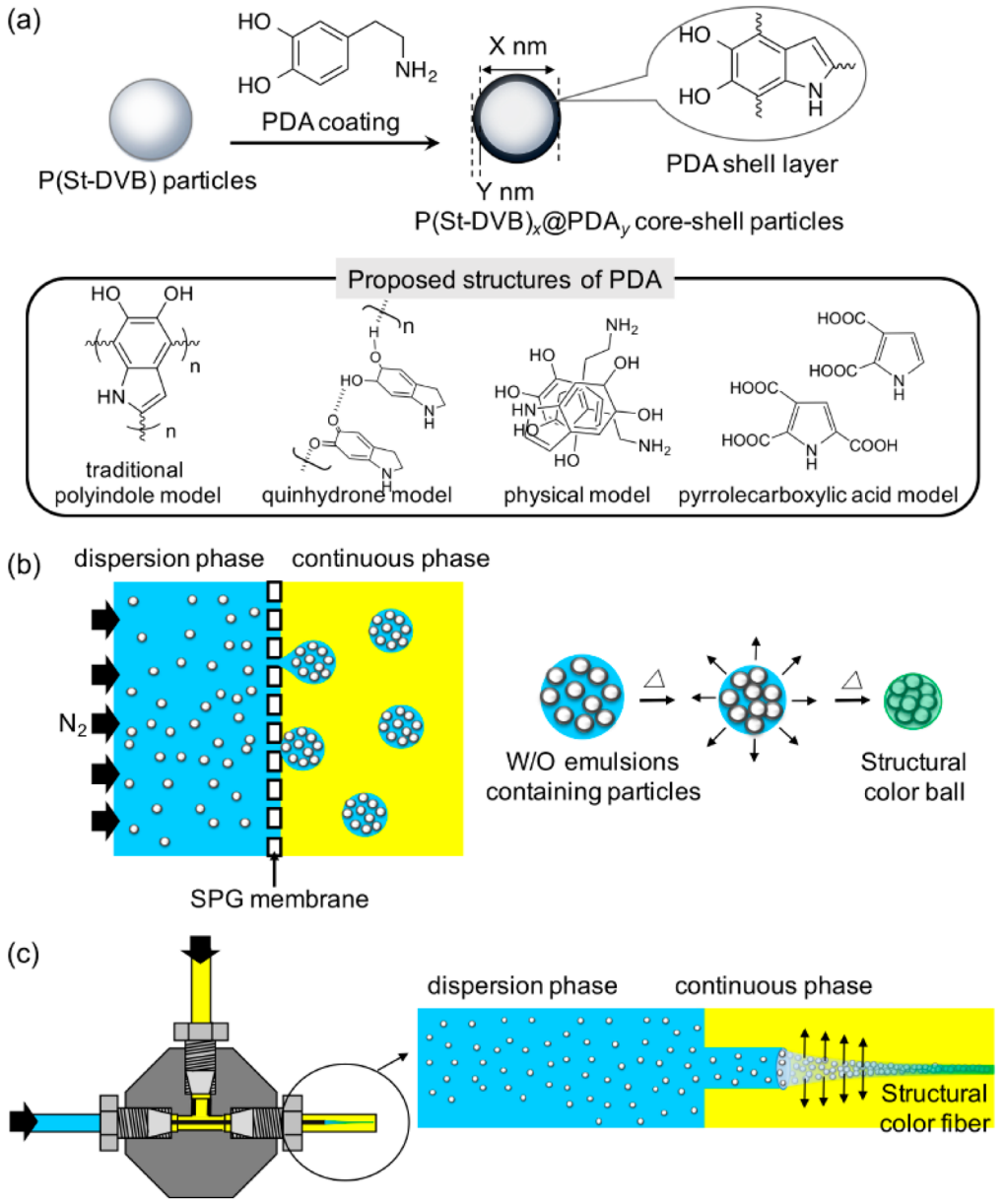


**Figure 1.** (a) Schematic representation of the fabrication of core−shell particles with biomimetic melanin-like PDA shell layers and some proposed structures of PDA. (b) Preparation of structural color balls through SPG membrane-assisted W/O emulsion synthesis followed by evaporation of water. (c) Preparation of structural color fibers by microfluidic emulsification and solvent diffusion.

of a polystyrene (PSt) core and PDA shell to create structural color materials in the solid state.[36] By controlling the diameters of the PSt core particles and the PDA shell thickness, we were able to obtain nearly the full range of structural colors with iridescent and noniridescent colors.[36] Films obtained from the PSt@PDA core−shell particles showed bright structural colors independent of background color.[37] Furthermore, the neutral structural colors could be successfully obtained by simply mixing two differently sized PSt@PDA core−shell particles.[38] In these reports, PDA is used as a mimetic of melanin, which is produced by several enzymatic reactions of 3,4-dihydroxyphenylalanine (DOPA) and is one of the primary components of nanostructural elements that produces structural coloration.[39−41] Biomimetic PDA-based particles act both as components of structural color materials and as scattering absorbers, producing structural colors. The structure of PDA is complex, and the work is still continuing. As shown in Figure 1a, some reports have been published for the PDA structures including a traditional polyindole model, quinhydrone model,[5] physical model,[42] and pyrrolecarboxylic acid model.[43]

In this forum article, we demonstrated the fabrication of three-dimensional (3D) colloidal photonic materials, i.e., structural color balls and fibers, from biomimetic core−shell particles with PDA shell layers (Figure 1). Many techniques have been reported to create emulsions containing colloidal particles to fabricate spherical colloidal crystals, such as electrospray devices,[44,45] double templating,[46] micropipette injection,[47] and microfluidic technology.[48,49] Since the Shirasu porous glass (SPG) membrane emulsification technique is a simple and useful technique to produce uniform emulsions compared with these techniques,[50] we prepared structural color balls through SPG membrane-assisted W/O emulsion synthesis followed by evaporation of water. For structural color fibers, few studies have focused on their fabrication by electro-


DOI: 10.1021/acsami.7b03453
ACS Appl. Mater. Interfaces XXXX, XXX, XXX−XXX

spinning.[51−53] Some of the present authors have reported facile preparation methods for colloidal assemblies based on microfluidic emulsification and solvent diffusion.[54−58] Thus, we demonstrated the preparation of structural color fibers created by applying microfluidic emulsification and solvent diffusion. To prepare structural color balls or fibers, it is required to use organic solvents as a continuous phase. PDA is not dissolved in these solvents because PDA is a cross-linking polymer. To prevent core particles from dissolving in the presence of organic solvents, we prepared polystyrene−divinylbenzene (P(St-DVB)) particles as a core material because DVB is usually used as comonomers for the synthesis of highly cross-linked polymers. Both structural color balls and fibers obtained showed angle-independent structural colors. The 3D colloidal photonic materials with angle-independent properties will provide a step toward the development of dye-free coloration strategies for inks, textiles, and other practical applications.

## EXPERIMENTAL SECTION

**Materials.** Dopamine hydrochloride (DA) was obtained from Sigma-Aldrich. Styrene (St), tris(hydroxymethyl)aminomethane (Tris), polyvinylpyrrolidone (PVP; M.W. 90,000), and tetrahydrofuran (THF) were obtained from Kanto Chemical. Divinylbenzene (DVB) was purchased from Nippon Steel and Sumikin Chemical. 2,2′-Azobis(2-amidinopropane) dihydrochloride (V50) and dodecane were obtained from Wako Pure Chemical. Span 85 was purchased from Tokyo Chemical Industry. Deionized water with a resistance of 18.2 MΩ·cm was obtained by passing through a Millipore Simplicity UV system. The hydrophilic comonomer *N*-*n*-butyl-*N*-2-methacryloyloxyethyl-*N*,*N*-dimethylammonium bromide ($C_4$DMAEMA) was synthesized according to the method reported in the literature.[36] St and DVB were dried over calcium hydride and distilled under reduced pressure. All other chemicals and solvents were of reagent grade and were used as received. A Shirasu porous glass (SPG) membrane (Cylindrical SPG membrane: 10 mm OD × 20 mm length, 20 μm pore size), which is a material in use mainly by Shirasu that is abundant in South Kyushu, was obtained from SPG Technology.

**Measurements.** Scanning electron microscopy (SEM) micrographs of the samples were obtained using a scanning electron microscope (JSM-6510A; JEOL). Reflection spectroscopy was performed using a spectrophotometer (V-650; JASCO) equipped with a reflection spectroscopy unit (ARSV-732; JASCO) and a microscopic spectrophotometer (MSV-370; JASCO). Photographs of the samples were taken with a digital camera (OM-D, Olympus). Ultraviolet−visible (UV−vis) spectra were obtained using a spectrophotometer (U-3010; Hitachi).

**Synthesis of P(St-DVB) Core Particles.** The P(St-DVB) core particles were synthesized by emulsifier-free emulsion polymerization of St, DVB, and $C_4$DMAEMA. St (8.33 g, 80 mmol), DVB (0.21 g, 1.6 mmol), $C_4$DMAEMA (0−0.05567 g, 0−0.19 mmol, 0−0.24 mol % with respect to St), and V50 (0.22 g, 0.80 mmol) were placed into a three-necked flask filled with 30 mL of deionized water and deoxygenated by purging with nitrogen for 15 min. The polymerization was initiated by heating to 60 °C while stirring at 200 rpm in a nitrogen atmosphere. After 10 h, the P(St-DVB) core particles were separated and purified repeatedly by centrifugation (14,500 rpm for 60 min) and redispersion.

**Synthesis of P(St-DVB)@PDA Core−Shell Particles.** A schematic illustration of the synthesis of core−shell particles is shown in Figure 1a. DA (12 mg, 63 μmol), Tris (1.45 g, 12 mmol), and P(St-DVB) particles (0.12 g) were dispersed in deionized water (120 mL) and stirred for 20 h at room temperature. The pH for the PDA coating was 10.7. The core−shell particles were separated and purified repeatedly by centrifugation (14,500 rpm for 20 min) and redispersion. A summary of the P(St-DVB)@PDA core−shell particles obtained is shown in Table S1.

**Preparation of Structural Color Balls.** A schematic illustration of membrane emulsification is shown in Figure 1b. The dispersion of P(St-DVB)@PDA core−shell particles (2.5 wt %, 1 mL) was transferred to the water tank on the SPG membrane emulsification apparatus. The SPG membrane emulsification technique was initiated by streaming nitrogen gas into the water phase, which was conducted in a 20 mL bottle containing 13 mL of dodecane with span 85 (3 wt %). After preparing the W/O emulsion, structural color balls were prepared by solvent evaporation at 60 °C.

**Preparation of Structural Color Fibers.** A schematic illustration of the microfluidics is shown in Figure 1c. The microfluidic device was fabricated by assembling a stainless steel (SUS) tube (inside: 130 μm, outside: 310 μm), fluorinated ethylene propylene (FEP) tubes (inside: 500 μm), and a T-shaped union, according to a previous report with some modifications.[54] A water dispersion of P(St-DVB)234@$PDA_4$ core−shell particles (5 wt %) and PVP solution (5 wt %, $M_w$: 90,000) (6/1(v/v)) was used as the inner solution (dispersed phase). THF was used as a continuous phase. The flow rates of the inner and outer fluids were typically set to 3 and 400 μL/min, respectively, using syringe pumps. The structural color fibers were precipitated by diffusion of water in the inner solution to THF in the continuous phase at the exit of the inner tube.

## RESULTS AND DISCUSSION

**Synthesis of P(St-DVB)@PDA Core−Shell Particles.** First, P(St-DVB) core particles were prepared by emulsifier-free emulsion polymerization of St in the presence of DVB and hydrophilic comonomer ($C_4$DMAEMA), which was added to control the core particle diameter.[36] The amount of added $C_4$DMAEMA was varied in the range of 0−0.24 mol % with respect to St. The diameter of particles without $C_4$DMAEMA was determined to be approximately 444 nm. As shown in Figure S1, the particle size was decreased with increasing the $C_4$DMAEMA feed concentration; this is a general trend that has been observed in emulsifier-free emulsion polymerization in the presence of hydrophilic comonomers. When increasing the concentration of highly reactive and water-soluble comonomers, the number of particles increases, and as a consequence, the particle size decreases.[59] P(St-DVB) core particles with different diameters (184, 234, and 262 nm), which were prepared in the presence of $C_4$DMAEMA (0.24, 0.16, and 0.13 mol % with respect to St, respectively), were used as samples for preparing core−shell particles.

Next, P(St-DVB)@PDA core−shell particles were prepared by DA polymerization in the presence of P(St-DVB) particles.[36] The synthesized products were designated P(St-DVB)$_x$@PDA$_y$ core−shell particles (*x*, diameter of P(St-DVB) core particles; *y*, thickness of PDA shell layer). As indicated in the SEM micrographs, the obtained P(St-DVB)$_{184}$@$PDA_{3.5}$, P(St-DVB)$_{234}$@$PDA_4$, and P(St-DVB)$_{262}$@$PDA_{3.5}$ core−shell particles displayed smooth spherical shapes (Figure 2a) as well as core particles (Figure S2). In each sample, the sizes of 100 particles were measured using SEM to calculate the diameter of the particles. While the formation of PDA layers was not clarified by SEM measurements, the diameters of particles after PDA coatings were clearly increased compared with that of core particles (Table S1). PDA shell layers, calculated by the difference in core and core−shell particle diameters, were approximately 3.5−4 nm. The SEM images also showed the diameter distribution of the particle diameters in terms of the coefficient of variation (CV), which ranged from approximately 3.65% to 5.85%, indicating the formation of relatively monodisperse particles. The dispersions of P(St-DVB)@PDA core−shell particles (1.5 wt % in water) were brown in color due to absorption (Figure 2a, insets). To investigate the


DOI: 10.1021/acsami.7b03453
ACS Appl. Mater. Interfaces XXXX, XXX, XXX−XXX

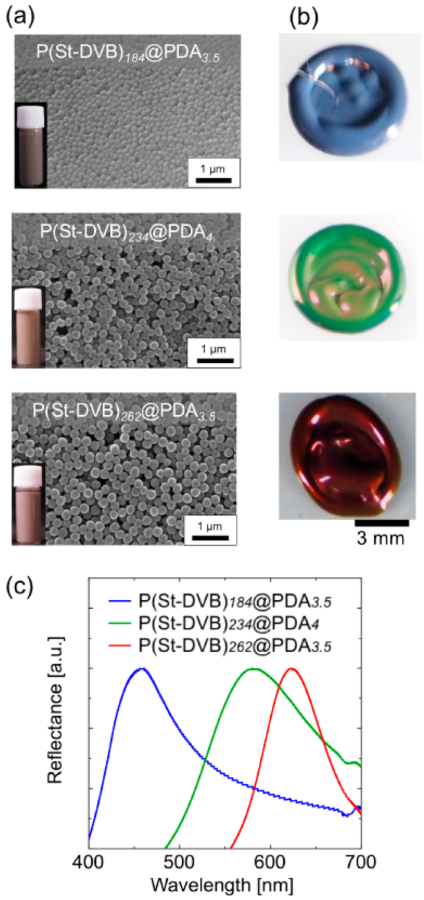


**Figure 2.** (a) SEM images of P(St-DVB)$_{184}$@PDA$_{3.5}$, P(St-DVB)$_{234}$@PDA$_4$, and P(St-DVB)$_{262}$@PDA$_{3.5}$ core−shell particles. Inset shows images of water dispersions of core−shell particles (5 wt %). (b) Photographs of structural color pellets prepared using P(St-DVB)$_{184}$@PDA$_{3.5}$, P(St-DVB)$_{234}$@PDA$_4$, and P(St-DVB)$_{262}$@PDA$_{3.5}$ core−shell particles. (c) Reflection spectra of pellets shown in b.

presence of PDA layers, we measured UV−vis absorbance spectra of P(St-DVB)$_{262}$ core particles and P(St-DVB)$_{262}$@PDA$_{3.5}$ core−shell particles together with PDA particles.[31] As shown in Figure S3, PDA absorbed the whole range of visible light. Unfortunately, the absorbance of the PDA layer in the spectrum of PDA-coated particles was not confirmed because of the scattering of light. Thus, pellets were prepared by pouring P(St-DVB) core particles or P(St-DVB)@PDA core−shell particle suspensions (solid contents: 10 wt %) onto a silicone rubber plate and allowing them to dry at room temperature for 12 h. While reflectance spectra of pellets from the core particles were clearly obtained, the pellets showed milky-white colors (Figure S4). In contrast, beautiful structural color pellets were obtained from PDA-coated core−shell particles because the PDA shell layers effectively absorbed light scattering, enhancing the structural coloration (Figure 2b), in agreement with our previously reported results.[36] This result clearly indicates the presence of PDA layers. As the diameter of the core−shell particles increased, the colors of the pellets changed from blue to green to red. Figure 2c shows the reflection spectra of the three pellets. Reflection peaks were red-shifted as the core−shell particle diameters increased, in agreement with a previously reported result.[36]

**Construction and Properties of Structural Color Balls.** Structural color balls were prepared using the SPG membrane emulsification technique. The water dispersion of P(St-DVB)$_{234}$@PDA$_4$ core−shell particles was transferred to the water tank on the SPG membrane emulsification apparatus. Then, SPG membrane emulsification was initiated by streaming nitrogen gas into the water phase. Dodecane in the presence of span 85 (surfactant) was used as the dispersed phase. After emulsification, W/O emulsions with a diameter of approximately 71 $\mu$m were obtained (Figure 3a). The optical microscopic image showed the emulsion diameter distributions, in terms of the CV, were approximately 10%, suggesting the formation of relatively monodisperse emulsions. The emulsions were used as a template for the generation of structural color balls. The W/O emulsions were transferred into a dish and

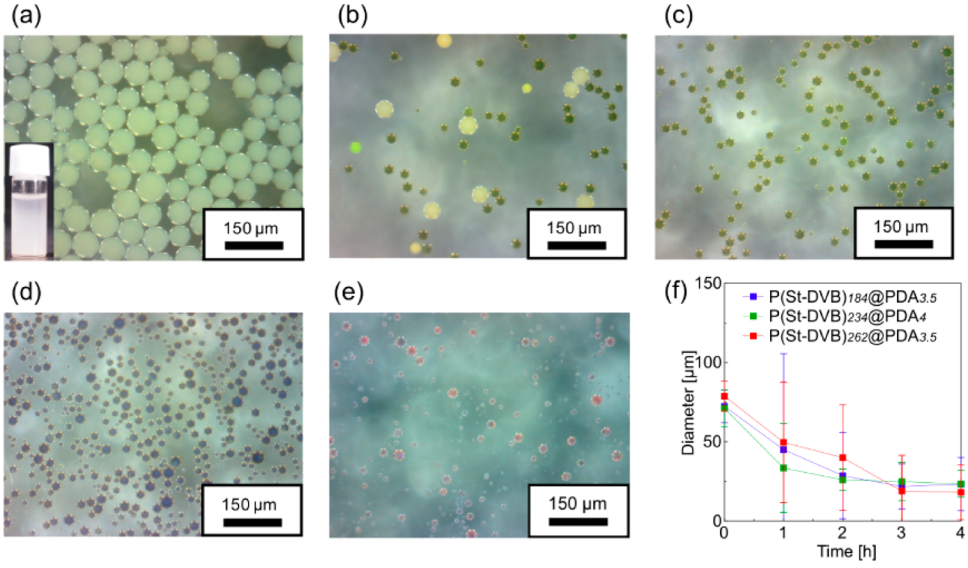


**Figure 3.** Optical microscope images of W/O emulsions containing P(St-DVB)$_{234}$@PDA$_4$ core−shell particles after heating for (a) 0 h (the inset shows the photograph of dodecane dispersions of W/O emulsions), (b) 1 h, and (c) 3 h. Optical microscope images of W/O emulsions containing (d) P(St-DVB)$_{184}$@PDA$_{3.5}$ (e) and P(St-DVB)$_{262}$@PDA$_{3.5}$ core−shell particles after heating for 3 h. (f) Diameter of the W/O emulsions as a function of heating time.


DOI: 10.1021/acsami.7b03453
ACS Appl. Mater. Interfaces XXXX, XXX, XXX−XXX

placed at 60 °C to evaporate water. As the dispersed phase (dodecane: boiling point 216 °C) was heated by a hot plate, the water in the W/O emulsions started to evaporate. Microscopic images of the condensation process of the emulsions showed a decrease in the diameter and color change, and green droplets were eventually observed (Figure 3b,c). During water evaporation, P(St-DVB)$_{234}$@PDA$_4$ core−shell particles were gradually self-assembled, and structural colors appeared. While the W/O emulsions were white due to light scattering (Figure 3a, inset), structural colors were observed when the water was completely evaporated (Figure 4b). In the same manner, blue

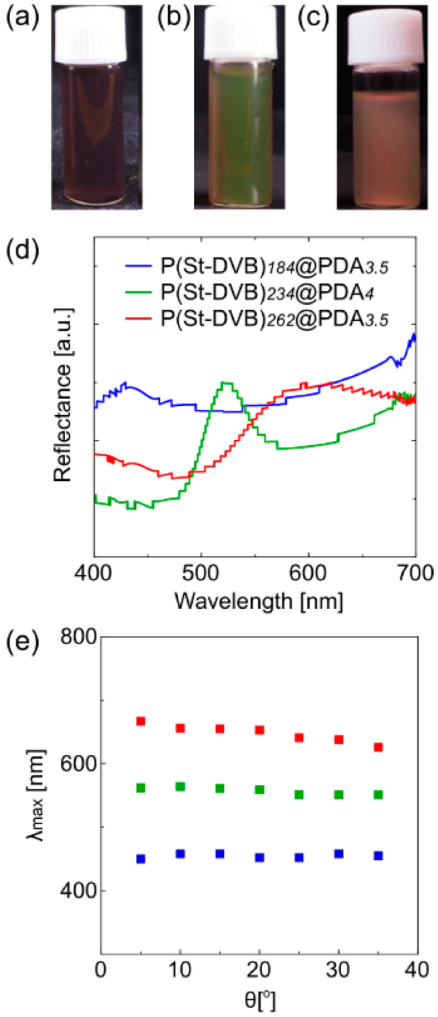


**Figure 4.** Photographs of dodecane dispersions of structural color balls prepared using (a) P(St-DVB)$_{184}$@PDA$_{3.5}$, (b) P(St-DVB)$_{234}$@PDA$_4$, and (c) P(St-DVB)$_{262}$@PDA$_{3.5}$ core−shell particles. (d) Reflection spectra of pellets prepared from structural color balls. (e) Plots of $\lambda_{max}$ for the reflection spectra of the dodecane dispersions of structural color balls (P(St-DVB)$_{234}$@PDA$_4$) as a function of incident angle ($\theta$).

and red structural color balls were obtained from P(St-DVB)$_{184}$@PDA$_{3.5}$ and P(St-DVB)$_{262}$@PDA$_{3.5}$ core−shell particles, respectively (Figure 3d,e and Figure 4a,c). As shown in Figure 3f, the W/O emulsion diameters, which were measured using microscopic images, gradually decreased from approximately 70 $\mu$m and reached a plateau of approximately 20 $\mu$m after 3 h, regardless of the type of core−shell particle. The CVs of the structural color balls were approximately 15%, indicating that the P(St-DVB)@PDA core−shell particle assemblies could form structural color balls with lower polydispersity. The structural color balls were stable in dodecane because P(St-DVB)@PDA core−shell particles were not dispersed in dodecane. Although the balls settled at the bottom due to their weight, they were easily redispersed. To investigate the usability of the use of PDA-coated particles, balls from P(St-DVB)$_{262}$ core particles were prepared by the same process. As shown in Figure S5a, W/O emulsions with approximately 70 $\mu$m in diameter from P(St-DVB)$_{262}$ core particles were also obtained. Although balls composed of P(St-DVB) core particles were successfully observed after the evaporation of water, they showed milky-white colors due to light scattering in the naked eye (Figure S5b). In contrast, balls from PDA-coated P(St-DVB) particles showed structural colors because PDA shell layers effectively absorbed the light scattering, enhancing the structural coloration (*vide supra*). These control experiments clearly indicated the usefulness of PDA coating.

The reflectance spectra of each structural color ball dispersed in dodecane were measured using a microscopic spectrophotometer (Figure 4d). The spectrum of the blue dispersion that was prepared by P(St-DVB)$_{184}$@PDA$_{3.5}$ core−shell particles had a clear reflection peak at approximately 429 nm. The $\lambda_{max}$ values of the reflection peaks of the green and red dispersions that were prepared by P(St-DVB)$_{234}$@PDA$_4$ and P(St-DVB)$_{262}$@PDA$_{3.5}$ core−shell particles were approximately 519 and 621 nm, respectively, indicating that the reflection peaks increased with increasing diameter of the core−shell particles. Under normal incidence, the peak value was estimated based on Bragg's law (eq 1).[60]

$$m\lambda = \sqrt{\frac{8}{3}d^2\left(\sum_i n_i^2 V_i - \sin^2\theta\right)} \quad (1)$$

where $m$ is the order of diffraction, $\lambda$ is the wavelength of light, $n_i$ and $V_i$ are, respectively, the refractive index and volume fraction of each component, $d$ is the center-to-center distance between the nearest particles, and $\theta$ is the angle between the incident light and the diffraction crystal planes. The reflection wavelength was calculated using eq 1 assuming that Bragg's law holds ($m$ = 1, $\theta$ = 90, and $d$ is the diameter of P(St-DVB)$_x$@PDA$_y$ core−shell particles). The refractive index ($n$) is the effective refractive index of the particle/dodecane composite. The packing factor is 0.74 as in the closely packed faced-centered cubic (FCC) structure. Therefore, $\sum_i n_i^2 V_i = 0.74 \cdot n_p^2 + 0.26 \cdot n_s^2$, where $n_p$ and $n_s$ are the refractive indices of P(St-DVB)@PDA core−shell particles and solvent (dodecane: $n_s$ = 1.42), respectively. While the refractive index of the P(St-DVB)@PDA core−shell particles was unknown, our most recent evidence indicates that the refractive index of PDA-covered particles with thin shell layers (0−4.5 nm) is relatively the same as the refractive index of core particles.[36] Thus, the refractive index of the P(St-DVB)@PDA core−shell particles ($n_p$) was set to 1.59. The reflection wavelengths for balls prepared by P(St-DVB)$_{184}$@PDA$_{3.5}$, P(St-DVB)$_{234}$@PDA$_4$, and P(St-DVB)$_{262}$@PDA$_{3.5}$ core−shell particles were estimated at approximately 368, 467, and 519 nm, respectively, which were slightly smaller than the actual values (*vide supra*). This phenomenon is probably due to the difference of packing structures and the swelling of core−shell particles in dodecane. In the present experiment, the highest reflectance was approximately 7%, and the reflectivity was not influenced by the size of the structural color balls or the core−shell particle diameter. Although reflectivity was relatively low, PDA shell layers effectively


DOI: 10.1021/acsami.7b03453
ACS Appl. Mater. Interfaces XXXX, XXX, XXX−XXX

absorbed scattered light, producing structural color balls that could be seen with the naked eye.

We also measured the reflectivity of the sample dispersions at various angles by rotating the detection stage. As shown in Figure 4e, the spectral shifts of the reflection spectra taken at several different angles of the P(St-DVB)$_{184}$@PDA$_{3.5}$, P(St-DVB)$_{234}$@PDA$_4$, and P(St-DVB)$_{262}$@PDA$_{3.5}$ core−shell particles in quartz cells were small, indicating that the structural colors from the balls obtained were angle-independent. From previous reports, the angle dependency of structural colors depends on the arrangement of the colloidal particles.[36,61,62] Thus, to investigate the arrangement of core−shell particles, we performed SEM measurements on the structural color balls. The SEM samples were prepared from the dispersion of balls after solvent exchange from dodecane to hexane. Figure 5

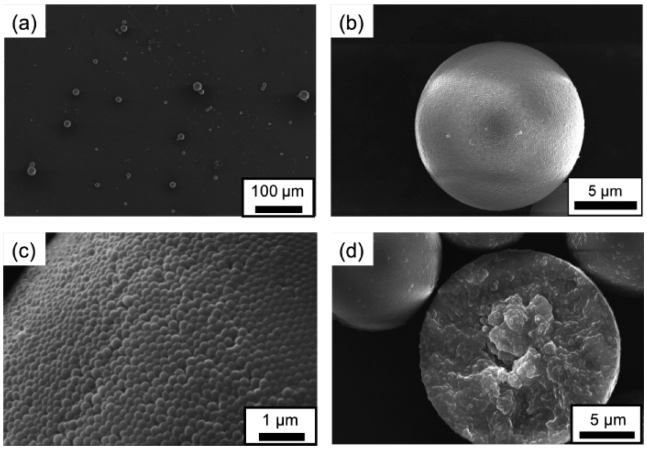


**Figure 5.** (a−c) SEM images of structural color balls (P(St-DVB)$_{234}$@PDA$_4$). (d) Cross-section view of the structural color balls (P(St-DVB)$_{234}$@PDA$_4$).

shows the SEM images of the structural color balls obtained from P(St-DVB)$_{234}$@PDA$_4$ core−shell particles. As shown in Figure 5a−c, the balls were generally spherical with smooth surfaces. For cross-section SEM measurements, the balls were deliberately broken by a spatula. As shown in Figure 5d, the cross-section of the balls showed the densely packed structure of particles. Several studies have reported that there are two types of structural color.[36,61,62] Angle-dependent structural colors are obtained from colloidal crystal structures, which are close-packed structures, and angle-independent colors are obtained from amorphous structures that show roughly packed arrays. Usually, a Fourier transform (FFT) of the SEM images of particles is performed to obtain their spatial information. While sharp hexagonal peaks are observed from colloidal crystal structures, circular patterns are obtained from amorphous structures.[36,61] Thus, we performed the FFT of the SEM images (Figure 5c) from the samples. Unfortunately, clear patterns were not observed because elliptical FFT indicates astigmatism. However, it seems that obtained SEM images showed the formation of the amorphous structures. In the present experiment, while PDA coatings with a thin thickness could produce uniform samples, the CVs of the P(St-DVB)@PDA core−shell particles were approximately 3.89−5.85% due to the P(St-DVB) core particles (approximately 3.65−4.97%). Usually, the addition of DVB broadens the particle size distribution.[63] The use of relatively monodisperse P(St-DVB)@PDA core−shell particles prevented the formation of colloidal crystals and created amorphous colloidal structures. The surface roughness of the PDA layer may also influence the formation of amorphous structures. Typically, the PDA coating provides a somewhat rough coating as described in previous research.[64] In the amorphous state, diffraction is suppressed, and the reflection spectra related to the size of the particles are selectively enhanced, producing angle-independent structural colors.[36,61] These properties are useful to produce new generation color materials, such as photonic reflective displays.

**Construction and Properties of Structural Color Fibers.** The construction of 3D photonic crystal materials, such as fibers, is an important application. We prepared structural color fibers from P(St-DVB)@PDA core−shell particles. Both an inner aqueous solution consisting of a dispersion of P(St-DVB)$_{234}$@PDA$_4$ core−shell particles (5 wt %) and PVP (5 wt %) and a continuous outer fluid (THF) were separately injected from the inner tube and outer tube. The ratio of a water dispersion of core−shell particles and PVP solution was set at 6/1. When the coaxial laminar flow of the two fluids merged at the exit of the inner tube, stable W/O jetting flow was formed because of the miscibility between water and THF. Then, water in the inner fluid started to diffuse into THF in the outer fluid. Since P(St-DVB)@PDA core−shell particles were not dispersed in THF and PVP was not dissolved in THF, fiber-structured materials composed of core−shell particles and PVP were obtained during solvent diffusion of water into THF. We already found that solvent diffusion in the microfluidic device occurred within a few seconds.[55,56] When the core−shell particle dispersion without PVP was used as the dispersed phase, fibers were not obtained, indicating the importance of PVP for fiber formation. In the present method, fibers were obtained from dispersed phase by a solvent diffusion process. Since diffusion rapidly occurred, it will be required that the dispersed phase stably exists on the line. While we believe that PVP concentration is one of the key factors in the formation of fiber shape, to obtain stable lines due to their viscosity, more detailed experiments will need to be conducted to obtain detailed mechanisms.

SEM images show the presence of fibers with an average diameter of 10 μm (Figure 6a,b). Almost no cracks were formed in the fibers, indicating the flexibility of the fibers. The cross-sectional view (Figure 6c) and enlarged view (Figure 6d) of the SEM images clearly indicated the presence of closely packed core−shell particles, and the arrangements of particles were amorphous structures. The fibers were dried on glass substrates, and green structural color fibers were obtained (Figure 6e). As shown in Figure 6f, the reflection spectrum of the structural color fibers showed green color. To investigate the concentration of PVP, the ratio of the water dispersion of core−shell particles and PVP solution was varied at 6/1, 8/1, and 10/1 (v/v). While fibers obtained were easily broken as PVP concentration decreased, fibers were observed in the present experimental conditions (Figure S6). Although a detailed study of fiber preparation might be necessary to obtain more vivid structural colors, our results demonstrate that flexible structural color fibers composed of core−shell particles were successfully prepared by microfluidic emulsification and the solvent diffusion technique. While the electrospinning method is useful to fabricate polymeric fibers, it requires high voltage. On the other hand, the current method based on microfluidic emulsification and solvent diffusion is safe and easy to spin without using high voltage compared with the conventional electrospinning method. Furthermore, nonwoven


DOI: 10.1021/acsami.7b03453
ACS Appl. Mater. Interfaces XXXX, XXX, XXX−XXX

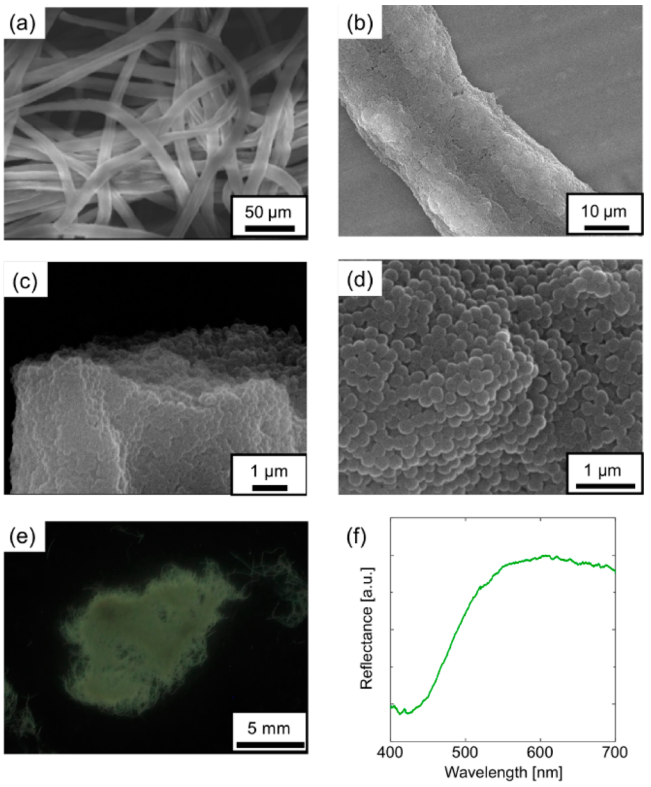


**Figure 6.** (a–d) SEM images and (e) a digital camera image of the structural color fibers prepared from P(St-DVB)$_{234}$@PDA$_4$) core–shell particles. (f) Reflection spectrum of the structural color fibers prepared from P(St-DVB)$_{234}$@PDA$_4$) core–shell particles.

fabrics are usually obtained by the electrospinning method. In contrast, the current method enables one to produce the sample as a single fiber, and it will be possible to wind up the samples.

## CONCLUSION

In summary, we developed angle-independent 3D colloidal photonic materials, i.e., structural color balls and fibers, from biomimetic core–shell particles with melanin-like PDA shell layers. By selecting the size of the PSt@PDA core–shell particles, blue, green, and red structural color balls were prepared using SPG membrane-assisted W/O emulsion synthesis followed by evaporation of water. Structural color balls obtained were created by the close-packed structure of the particles and had spherical shapes and smooth surfaces. In previous reports, since structural colored materials were preparing by simply assembling PDA particles or PSt@PDA core–shell particles, the colors disappeared as the structure of assembled materials collapsed. On the other hand, we prepared 3D structural color balls from dispersion of P(St-DVB)@PDA core–shell particles in the present forum article. In comparison with previous works, the present method enabled the creation of structural colors with balls dispersed in solvent since assembled structures of particles in balls remained. These characteristics will be useful to develop structural color based ink applications. Furthermore, we successfully demonstrated the synthesis of structural color fibers with flexible properties through microfluidic emulsification and solvent diffusion. This method will enable one to prepare a single fiber, and it will be possible to wind up the fibers. These properties will be useful to apply the samples for some applications such as in textiles. In the present methods, PDA shell layers effectively acted as light-scattering absorbers, producing structural color materials. This new type of PDA-based material is a promising tool for preparing 3D colloidal photonic materials since they are useful for practical applications. The structural color balls and fibers will be used as pigments, displays, sensors, and light diffusers.

## ASSOCIATED CONTENT

### Supporting Information

The Supporting Information is available free of charge on the ACS Publications website at DOI: 10.1021/acsami.7b03453.

Experimental details of synthetic procedures of particles and characterization and properties of structural color materials (PDF)

## AUTHOR INFORMATION

### Corresponding Author

*E-mail: kohri@faculty.chiba-u.jp.

### ORCID

Michinari Kohri: 0000-0003-1118-5568

### Notes

The authors declare no competing financial interest.

## ACKNOWLEDGMENTS

M.K. acknowledges the support of a JSPS KAKENHI (Grant Number 15H01593) in Scientific Research on Innovative Areas "Innovative Materials Engineering Based on Biological Diversity", the Noguchi Institute, Konica Minolta Science and Technology Foundation, and a Chiba University Venture Business Laboratory project. T.O. acknowledges the support by Industrial Technology Research Grant Program in 2011 from New Energy and Industrial Technology Development Organization (NEDO) of Japan.

## REFERENCES

(1) Lee, H.; Dellatore, S. M.; Miller, W. M.; Messersmith, P. B. Mussel-Inspired Surface Chemistry for Multifunctional Coatings. *Science* **2007**, *318*, 426–430.

(2) Lynge, M. E.; van der Westen, R.; Postma, A.; Städler, B. Polydopamine-a Nature-Inspired Polymer Coating for Biomedical Science. *Nanoscale* **2011**, *3*, 4916–4928.

(3) Kang, S. M.; Hwang, N. S.; Yeom, J.; Park, S. Y.; Messersmith, P. B.; Choi, I. S.; Langer, R.; Anderson, D. G.; Lee, H. One-Step Multipurpose Surface Functionalization by Adhesive Catecholamine. *Adv. Funct. Mater.* **2012**, *22*, 2949–2955.

(4) Guo, L.; Liu, Q.; Li, G.; Shi, J.; Liu, J.; Wang, T.; Jiang, G. A Mussel-Inspired Polydopamine Coating as a Versatile Platform for the *in situ* Synthesis of Graphene-Based Nanocomposites. *Nanoscale* **2012**, *4*, 5864–5867.

(5) Dreyer, D. R.; Miller, D. J.; Freeman, B. D.; Paul, D. R.; Bielawski, C. W. Elucidating the Structure of Poly(dopamine). *Langmuir* **2012**, *28*, 6428–6435.

(6) Zhang, X.; Wang, S. Q.; Xu, L.; Feng, L.; Ji, Y.; Tao, L.; Li, S.; Wei, Y. Biocompatible Polydopamine Fluorescent Organic Nanoparticles: Facile Preparation and Cell Imaging. *Nanoscale* **2012**, *4*, 5581–5584.

(7) Yang, Z.; Tu, Q.; Zhu, Y.; Luo, R.; Li, X.; Xie, Y.; Maitz, M. F.; Wang, J.; Huang, N. Mussel-Inspired Coating of Polydopamine Directs Endothelial and Smooth Muscle Cell Fate for Re-Endothelialization of Vascular Devices. *Adv. Healthcare Mater.* **2012**, *1*, 548–559.

(8) Ahn, M.; Kim, J. Electrochemical Behavior of Dopamine and Ascorbic Acid at Dendritic Au Rod Surfaces: Selective Detection of



DOI: 10.1021/acsami.7b03453
*ACS Appl. Mater. Interfaces* XXXX, XXX, XXX–XXX

Dopamine in the Presence of High Concentration of Ascorbic Acid. *J. Electroanal. Chem.* **2012**, *683*, 75−79.
(9) Ambrico, M.; Ambrico, P. F.; Cardone, A.; Della Vecchia, N. F.; Ligonzo, T.; Cicco, S. R.; Mastropasqua Talamo, M.; Napolitano, A.; Augelli, V.; Farinola, G. M.; d'Ischia, M. Engineering Polydopamine Films with Tailored Behavior for Next-Generation Eumelanin-Related Hybrid Devices. *J. Mater. Chem. C* **2013**, *1*, 1018−1028.
(10) Dreyer, D. R.; Miller, D. J.; Freeman, B. D.; Paul, D. R.; Bielawski, C. W. Perspectives on Poly(dopamine). *Chem. Sci.* **2013**, *4*, 3796−3802.
(11) Chen, X.; Yan, Y.; Müllner, M.; van Koeverden, M. P.; Noi, K. F.; Zhu, W.; Caruso, F. Engineering Fluorescent Poly(dopamine) Capsules. *Langmuir* **2014**, *30*, 2921−2925.
(12) Kim, Y. J.; Wu, W.; Chun, S. E.; Whitacre, J. F.; Bettinger, C. J. Catechol-Mediated Cycling Stability in Secondary Mg Batteries Using Eumelanin Cathodes. *Adv. Mater.* **2014**, *26*, 6572−6579.
(13) Liu, Y.; Ai, K.; Lu, L.; Polydopamine. and Its Derivative Materials: Synthesis and Promising Applications in Energy, Environmental, and Biomedical Fields. *Chem. Rev.* **2014**, *114*, 5057−5115.
(14) Guardingo, M.; Esplandiu, M. J.; Ruiz-Molina, D. Synthesis of Polydopamine at the Femtoliter Scale and Confined Fabrication of Ag Nanoparticles on Surfaces. *Chem. Commun.* **2014**, *50*, 12548−12551.
(15) Park, H. J.; Yang, K.; Kim, M. J.; Jang, J.; Lee, M.; Kim, D. W.; Lee, H.; Cho, S. W. Bio-Inspired Oligovitronectin-Grafted Surface for Enhanced Self-Renewal and Long-Term Maintenance of Human Pluripotent Stem Cells under Feeder-Free Conditions. *Biomaterials* **2015**, *50*, 127−139.
(16) Zhou, J.; Wang, C.; Wang, P.; Messersmith, P. B.; Duan, H. Multifunctional magnetic nanochains: Exploiting Self-Polymerization and Versatile Reactivity of Mussel-Inspired Polydopamine. *Chem. Mater.* **2015**, *27*, 3071−3076.
(17) Nair, B. G.; Hagiwara, K.; Ueda, M.; Yu, H. H.; Tseng, H. R.; Ito, Y. High Density of Aligned Nanowire Treated with Polydopamine for Efficient Gene Silencing by siRNA According to Cell Membrane Perturbation. *ACS Appl. Mater. Interfaces* **2016**, *8*, 18693−18700.
(18) Park, S. H.; Kim, H. J.; Lee, J.; Jeong, Y. K.; Choi, J. W.; Lee, H. Mussel-Inspired Polydopamine Coating for Enhanced Thermal Stability and Rate Performance of Graphite Anodes in Li-Ion Batteries. *ACS Appl. Mater. Interfaces* **2016**, *8*, 13973−13981.
(19) Ang, J. M.; Du, Y.; Tay, B. Y.; Zhao, C.; Kong, J.; Stubbs, L. P.; Lu, X. One-Pot Synthesis of Fe(III)−Polydopamine Complex Nanospheres: Morphological Evolution, Mechanism, and Application of the Carbonized Hybrid Nanospheres in Catalysis and Zn−Air Battery. *Langmuir* **2016**, *32*, 9265−9275.
(20) Mrówczyński, R.; Jurga-Stopa, J.; Markiewicz, R.; Coy, E. L.; Jurga, S.; Woźniak, A. Assessment of Polydopamine Coated Magnetic Nanoparticles in Doxorubicin Delivery. *RSC Adv.* **2016**, *6*, 5936−5943.
(21) Zhang, C.; Ou, Y.; Lei, W. X.; Wan, L. S.; Ji, J.; Xu, Z. K. $CuSO_4/H_2O_2$-Induced Rapid Deposition of Polydopamine Coatings with High Uniformity and Enhanced Stability. *Angew. Chem.* **2016**, *128*, 3106−3109.
(22) Feng, Y.; Zheng, Y.; Rahman, Z. U.; Wang, D.; Zhou, F.; Liu, W. Paper-Based Triboelectric Nanogenerators and Their Application in Self-Powered Anticorrosion and Antifouling. *J. Mater. Chem. A* **2016**, *4*, 18022−18030.
(23) Ponzio, F.; Barthès, J.; Bour, J.; Michel, M.; Bertani, P.; Hemmerlé, J.; d'Ischia, M.; Ball, V. Oxidant Control of Polydopamine Surface Chemistry in Acids: A Mechanism-Based Entry to Superhydrophilic-Superoleophobic Coatings. *Chem. Mater.* **2016**, *28*, 4697−4705.
(24) Kohri, M.; Kohma, H.; Shinoda, Y.; Yamauchi, M.; Yagai, S.; Kojima, T.; Taniguchi, T.; Kishikawa, K. A Colorless Functional Polydopamine Thin Layer as a Basis for Polymer Capsules. *Polym. Chem.* **2013**, *4*, 2696−2702.
(25) Kohri, M.; Shinoda, Y.; Kohma, H.; Nannichi, Y.; Yamauchi, M.; Yagai, S.; Kojima, T.; Taniguchi, T.; Kishikawa, K. Facile Synthesis of Free-Standing Polymer Brush Films Based on a Colorless Polydopamine Thin Layer. *Macromol. Rapid Commun.* **2013**, *34*, 1220−1224.
(26) Kohma, H.; Uradokoro, K.; Kohri, M.; Taniguchi, T.; Kishikawa, K. Hierarchically Structured Coatings by Colorless Polydopamine Thin Layer and Polymer Brush Layer. *Trans. Mater. Res. Soc. Jpn.* **2014**, *39*, 157−160.
(27) Kohri, M.; Kohma, H.; Uradokoro, K.; Taniguchi, T.; Kishikawa, K. Fabrication of Colored Particles Covered by Dye-Bearing Colorless Polydopamine Layer. *J. Colloid Sci. Biotechnol.* **2014**, *3*, 337−342.
(28) Kohri, M.; Nannichi, Y.; Kohma, H.; Abe, D.; Kojima, T.; Taniguchi, T.; Kishikawa, K. Size Control of Polydopamine Nodules Formed on Polystyrene Particles During Dopamine Polymerization with Carboxylic Acid-Containing Compounds for the Fabrication of Raspberry-Like Particles. *Colloids Surf., A* **2014**, *449*, 114−120.
(29) Kawamura, A.; Kohri, M.; Oku, H.; Hamada, K.; Nakagawa, K.; Taniguchi, T.; Kishikawa, K. Structural Color Materials from Polydopamine-Inorganic Hybrid Thin Films Inspired by Rock Pigeon Feathers. *Kobunshi Ronbunshu* **2017**, *74*, 54−58.
(30) Kohri, M.; Kawamura, A. Colorless Polydopamine Coatings for Creating Functional Interfaces. In *Polymer Science: Research Advances, Practical Applications and Educational Aspects*; Mendez-Vilas, A., Solano-Martín, A., Eds.; Formatex Research Center: Spain, 2016; pp 159−168.
(31) Kohri, M.; Nannichi, Y.; Taniguchi, T.; Kishikawa, K. Biomimetic Non-Iridescent Structural Color Materials from Polydopamine Black Particles that Mimic Melanin Granules. *J. Mater. Chem. C* **2015**, *3*, 720−724.
(32) Wu, T. F.; Hong, J. D. Dopamine-Melanin Nanofilms for Biomimetic Structural Coloration. *Biomacromolecules* **2015**, *16*, 660−666.
(33) Xiao, M.; Li, Y.; Allen, M. C.; Deheyn, D. D.; Xiujun Yue, X.; Zhao, J.; Gianneschi, N. C.; Shawkey, M. D.; Dhinojwala, A. Bio-Inspired Structural Colors Produced *via* Self-Assembly of Synthetic Melanin Nanoparticles. *ACS Nano* **2015**, *9*, 5454−5460.
(34) Xiao, M.; Li, Y.; Zhao, J.; Wang, Z.; Gao, M.; Gianneschi, N. C.; Dhinojwala, A.; Shawkey, M. D. Stimuli-Responsive Structurally Colored Films from Bioinspired Synthetic Melanin Nanoparticles. *Chem. Mater.* **2016**, *28*, 5516−5521.
(35) Cho, S.; Shim, T. S.; Kim, J. H.; Kim, D. H.; Kim, S. H. Selective Coloration of Melanin Nanospheres through Resonant Mie Scattering. *Adv. Mater.* **2017**, *29*, 1700256.
(36) Kawamura, A.; Kohri, M.; Morimoto, G.; Nannichi, Y.; Taniguchi, T.; Kishikawa, K. Full-Color Biomimetic Photonic Materials with Iridescent and Non-Iridescent Structural Colors. *Sci. Rep.* **2016**, *6*, 33984.
(37) Kohri, M.; Yamazaki, S.; Kawamura, A.; Taniguchi, T.; Kishikawa, K. Bright Structural Color Films Independent of Background Prepared by the Dip-Coating of Biomimetic Melanin-Like Particles Having Polydopamine Shell Layers. *Colloids Surf., A* **2017**, DOI: 10.1016/j.colsurfa.2017.03.035.
(38) Kawamura, A.; Kohri, M.; Yoshioka, S.; Taniguchi, T.; Kishikawa, K. Structural Color Tuning: Mixing Melanin-Like Particles with Different Diameters to Create Neutral Colors. *Langmuir* **2017**, *33*, 3824−3830.
(39) Yoshioka, S.; Kinoshita, S. Effect of Macroscopic Structure in Iridescent Color of the Peacock Feathers. *Forma* **2002**, *17*, 169−181.
(40) Zi, J.; Yu, X.; Li, Y.; Hu, X.; Xu, C.; Wang, X.; Liu, X.; Fu, R. Coloration Strategies in Peacock Feathers. *Proc. Natl. Acad. Sci. U. S. A.* **2003**, *100*, 12576−12578.
(41) Shawkey, M. D.; D'Alba, L.; Xiao, M.; Schutte, M.; Buchholz, R. Ontogeny of an Iridescent Nanostructure Composed of Hollow Melanosomes. *J. Morphol.* **2015**, *276*, 378−384.
(42) Hong, S.; Na, Y. S.; Choi, S.; Song, I. T.; Kim, W. Y.; Lee, H. Non-Covalent Self-Assembly and Covalent Polymerization Co-Contribute to Polydopamine Formation. *Adv. Funct. Mater.* **2012**, *22*, 4711−4717.
(43) Della Vecchia, N. F.; Avolio, R.; Alfè, M.; Errico, M. E.; Napolitano, A.; d'Ischia, M. Building-Block Diversity in Polydopamine Underpins a Multifunctional Eumelanin-Type Platform Tunable Through a Quinone Control Point. *Adv. Funct. Mater.* **2013**, *23*, 1331−1340.


DOI: 10.1021/acsami.7b03453
*ACS Appl. Mater. Interfaces* XXXX, XXX, XXX−XXX

(44) Moon, J. H.; Yi, G.-R.; Yang, S.-M.; Pine, D. J.; Park, S. B. Electrospray-Assisted Fabrication of Uniform Photonic Balls. *Adv. Mater.* **2004**, *16*, 605−609.
(45) Shen, Z.; Zhu, Y.; Wu, L.; You, B.; Zi, J. Fabrication of Robust Crystal Balls from the Electrospray of Soft Polymer Spheres/Silica Dispersion. *Langmuir* **2010**, *26*, 6604−6609.
(46) Klein, S. M.; Manoharan, V. N.; Pine, D. J.; Lange, F. F. Synthesis of Spherical Polymer and Titania Photonic Crystallites. *Langmuir* **2005**, *21*, 6669−6674.
(47) Rastogi, V.; Melle, S.; Calderón, O. G.; García, A. A.; Marquez, M.; Velev, O. D. Synthesis of Light-Diffracting Assemblies from Microspheres and Nanoparticles in Droplets on a Superhydrophobic Surface. *Adv. Mater.* **2008**, *20*, 4263−4268.
(48) Yi, G. R.; Manoharan, V. N.; Klein, S.; Brzezinska, K. R.; Pine, D. J.; Lange, F. F.; Yang, S. M. Monodisperse Micrometer-Scale Spherical Assemblies of Polymer Particles. *Adv. Mater.* **2002**, *14*, 1137−1140.
(49) Shang, L.; Fu, F.; Cheng, Y.; Wang, H.; Liu, Y.; Zhao, Y.; Gu, Z. Photonic Crystal Microbubbles as Suspension Barcodes. *J. Am. Chem. Soc.* **2015**, *137*, 15533−15539.
(50) Nakashima, T.; Shimizu, M.; Kukizaki, M. Membrane Emulsification by Microporous Glass. *Key Eng. Mater.* **1992**, *61*−*62*, 513−516.
(51) Liu, Z.; Zhang, Q.; Wang, H.; Li, Y. Structural Colored Fiber Fabricated by a Facile Colloid Self-Assembly Method in Micro-Space. *Chem. Commun.* **2011**, *47*, 12801−12803.
(52) Sun, X.; Zhang, J.; Lu, X.; Fang, X.; Peng, H. Mechanochromic Photonic-Cystal Fibers Based on Continuous Sheets of Aligned Carbon Nanotubes. *Angew. Chem., Int. Ed.* **2015**, *54*, 3630−3634.
(53) Yuan, W.; Zhou, N.; Shi, L.; Zhang, K. Q. Structural Coloration of Colloidal Fiber by Photonic Band Gap and Resonant Mie Scattering. *ACS Appl. Mater. Interfaces* **2015**, *7*, 14064−14071.
(54) Kamio, E.; Ono, T.; Yoshizawa, H. Design of a New Static Micromixer Having Simple Structure and Excellent Mixing Performance. *Lab Chip* **2009**, *9*, 1809−1812.
(55) Watanabe, T.; Ono, T.; Kimura, Y. Continuous Fabrication of Monodisperse Polylactide Microspheres by Droplet-To-Particle Technology Using Microfluidic Emulsification and Emulsion-Solvent Diffusion. *Soft Matter* **2011**, *7*, 9894−9897.
(56) Watanabe, T.; Kimura, Y.; Ono, T. Microfluidic Fabrication of Monodisperse Polylactide Microcapsules with Tunable Structures through Rapid Precipitation. *Langmuir* **2013**, *29*, 14082−14088.
(57) Watanabe, T.; Lopez, C. G.; Douglas, J. F.; Ono, T.; Cabral, J. T. Microfluidic Approach to the Formation of Internally Porous Polymer Particles by Solvent Extraction. *Langmuir* **2014**, *30*, 2470−2479.
(58) Watanabe, T.; Kimura, Y.; Ono, T. Monodisperse Polylactide Microcapsules with a Single Aqueous Core Prepared *via* Spontaneous Emulsification and Solvent Diffusion. *RSC Adv.* **2014**, *4*, 4872−4877.
(59) Sauzedde, F.; Ganachaud, F.; Elaïssari, A.; Pichot, C. Emulsifier-Free Emulsion Copolymerization of Styrene with Two Different Amino-Containing Monomers: II. Surface and Colloidal Characterization. *J. Appl. Polym. Sci.* **1997**, *65*, 2331−2342.
(60) Ge, J.; Yin, Y. Responsive Photonic Crystals. *Angew. Chem., Int. Ed.* **2011**, *50*, 1492−1522.
(61) Takeoka, Y. Angle-Independent Structural Coloured Amorphous Arrays. *J. Mater. Chem.* **2012**, *22*, 23299−23309.
(62) Takeoka, Y.; Yoshioka, S.; Takano, A.; Arai, S.; Nueangnoraj, K.; Nishihara, H.; Teshima, M.; Ohtsuka, Y.; Seki, T. Production of Colored Pigments with Amorphous Arrays of Black and White Colloidal Particles. *Angew. Chem., Int. Ed.* **2013**, *52*, 7261−7265.
(63) Song, J. S.; Winnik, M. A. Cross-Linked, Monodisperse, Micron-Sized Polystyrene Particles by Two-Stage Dispersion Polymerization. *Macromolecules* **2005**, *38*, 8300−8307.
(64) Hong, S.; Kim, J.; Na, Y. S.; Park, J.; Kim, S.; Singha, K.; Im, G. I.; Han, D. K.; Kim, W. J.; Lee, H. Poly(norepinephrine): Ultrasmooth Material-Independent Surface Chemistry and Nanodepot for Nitric Oxide. *Angew. Chem., Int. Ed.* **2013**, *52*, 9187−9191.


DOI: 10.1021/acsami.7b03453
*ACS Appl. Mater. Interfaces* XXXX, XXX, XXX−XXX